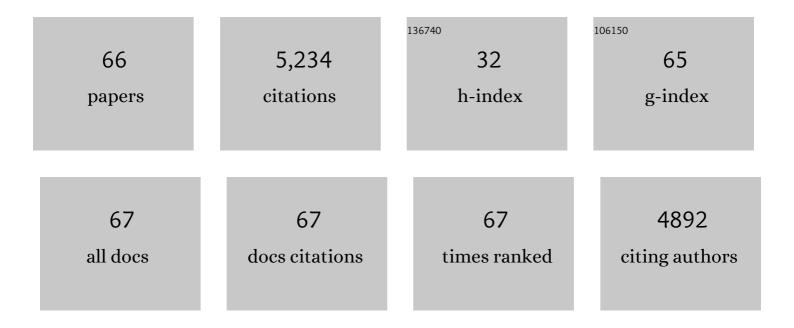
List of Publications by Year in descending order

Source: https://exaly.com/author-pdf/5307881/publications.pdf Version: 2024-02-01



Ромены Ун

#	Article	IF	CITATIONS
1	Fe–N–C electrocatalyst with dense active sites and efficient mass transport for high-performance proton exchange membrane fuel cells. Nature Catalysis, 2019, 2, 259-268.	16.1	958
2	Multifunctional Organic–Inorganic Hybrid Aerogel for Selfâ€Cleaning, Heatâ€Insulating, and Highly Efficient Microwave Absorbing Material. Advanced Functional Materials, 2019, 29, 1807624.	7.8	458
3	Porous CNTs/Co Composite Derived from Zeolitic Imidazolate Framework: A Lightweight, Ultrathin, and Highly Efficient Electromagnetic Wave Absorber. ACS Applied Materials & Interfaces, 2016, 8, 34686-34698.	4.0	427
4	Singleâ€Atom to Singleâ€Atom Grafting of Pt <sub>1</sub> onto FeN <sub>4</sub> Center: Pt <sub>1</sub> @FeNC Multifunctional Electrocatalyst with Significantly Enhanced Properties. Advanced Energy Materials, 2018, 8, 1701345.	10.2	371
5	Magnetically Aligned Co–C/MWCNTs Composite Derived from MWCNT-Interconnected Zeolitic Imidazolate Frameworks for a Lightweight and Highly Efficient Electromagnetic Wave Absorber. ACS Applied Materials & Interfaces, 2017, 9, 30850-30861.	4.0	282
6	Flexible nanocomposites with enhanced microwave absorption properties based on Fe <sub>3</sub> O <sub>4</sub> /SiO <sub>2</sub> nanorods and polyvinylidene fluoride. Journal of Materials Chemistry A, 2015, 3, 12197-12204.	5.2	165
7	Hierarchical NiCo <sub>2</sub> O <sub>4</sub> /Co <sub>3</sub> O <sub>4</sub> /NiO porous composite: a lightweight electromagnetic wave absorber with tunable absorbing performance. Journal of Materials Chemistry C, 2017, 5, 3770-3778.	2.7	161
8	lron atom–cluster interactions increase activity and improve durability in Fe–N–C fuel cells. Nature Communications, 2022, 13, .	5.8	159
9	Hydrogen storage in incompletely etched multilayer Ti2CTx at room temperature. Nature Nanotechnology, 2021, 16, 331-336.	15.6	145
10	Yolk–shell structured Co-C/Void/Co9S8 composites with a tunable cavity for ultrabroadband and efficient low-frequency microwave absorption. Nano Research, 2018, 11, 4169-4182.	5.8	139
11	Effects of local structure of Ce3+ ions on luminescent properties of Y3Al5O12:Ce nanoparticles. Scientific Reports, 2016, 6, 22238.	1.6	109
12	Controllable permittivity in 3D Fe <sub>3</sub> O <sub>4</sub> /CNTs network for remarkable microwave absorption performances. RSC Advances, 2017, 7, 26801-26808.	1.7	104
13	Efficient microwave absorber and supercapacitors derived from puffed-rice-based biomass carbon: Effects of activating temperature. Journal of Colloid and Interface Science, 2021, 594, 290-303.	5.0	99
14	Sequential Synthesis and Activeâ€Site Coordination Principle of Precious Metal Singleâ€Atom Catalysts for Oxygen Reduction Reaction and PEM Fuel Cells. Advanced Energy Materials, 2020, 10, 2000689.	10.2	92
15	Environmentally Tough and Stretchable MXene Organohydrogel with Exceptionally Enhanced Electromagnetic Interference Shielding Performances. Nano-Micro Letters, 2022, 14, 77.	14.4	91
16	Structure evolution of Prussian blue analogues to CoFe@C core–shell nanocomposites with good microwave absorbing performances. RSC Advances, 2016, 6, 105644-105652.	1.7	81
17	Hydrogen Passivation of M–N–C (M <b>=</b> Fe, Co) Catalysts for Storage Stability and ORR Activity Improvements. Advanced Materials, 2021, 33, e2103600.	11.1	81
18	Boosting electrocatalytic water splitting via metal-metalloid combined modulation in quaternary Ni-Fe-P-B amorphous compound. Nano Research, 2020, 13, 447-454.	5.8	77

#	Article	IF	CITATIONS
19	Antiferromagnetic Piezospintronics. Advanced Electronic Materials, 2019, 5, 1900176.	2.6	73
20	Recent advances in magnesium-based hydrogen storage materials with multiple catalysts. International Journal of Hydrogen Energy, 2019, 44, 10694-10712.	3.8	71
21	Enhanced high-frequency absorption of anisotropic Fe3O4/graphene nanocomposites. Scientific Reports, 2016, 6, 25075.	1.6	69
22	Effect of Ti substitution on hydrogen storage properties of Zr1â^'xTixCo (x = 0, 0.1, 0.2, 0.3) alloys. Journal of Energy Chemistry, 2014, 23, 9-14.	7.1	68
23	Synergy between metallic components of MoNi alloy for catalyzing highly efficient hydrogen storage of MgH2. Nano Research, 2020, 13, 2063-2071.	5.8	64
24	Hierarchical Cobalt Selenides as Highly Efficient Microwave Absorbers with Tunable Frequency Response. ACS Applied Materials & Interfaces, 2020, 12, 1222-1231.	4.0	62
25	Flaky FeSiAl alloy-carbon nanotube composite with tunable electromagnetic properties for microwave absorption. Scientific Reports, 2016, 6, 35377.	1.6	56
26	MWCNTs as Conductive Network for Monodispersed Fe <sub>3</sub> O <sub>4</sub> Nanoparticles to Enhance the Wave Absorption Performances. Advanced Engineering Materials, 2018, 20, 1700543.	1.6	50
27	An Efficient Co/C Microwave Absorber with Tunable Co Nanoparticles Derived from a ZnCo Bimetallic Zeolitic Imidazolate Framework. Particle and Particle Systems Characterization, 2018, 35, 1800107.	1.2	47
28	Surface-oxidized FeCo/carbon nanotubes nanorods for lightweight and efficient microwave absorbers. Materials and Design, 2017, 136, 13-22.	3.3	46
29	Surfactant-free synthesis of octahedral ZnO/ZnFe2O4 heterostructure with ultrahigh and selective adsorption capacity of malachite green. Scientific Reports, 2016, 6, 25074.	1.6	44
30	Fe <sub>3</sub> O <sub>4</sub> Nanoflower-Carbon Nanotube Composites for Microwave Shielding. ACS Applied Nano Materials, 2019, 2, 5475-5482.	2.4	42
31	A layered double hydroxide-derived exchange spring magnet array grown on graphene and its application as an ultrathin electromagnetic wave absorbing material. Journal of Materials Chemistry C, 2019, 7, 12270-12277.	2.7	42
32	Surface-Oxidized Amorphous Fe Nanoparticles Supported on Reduced Graphene Oxide Sheets for Microwave Absorption. ACS Applied Nano Materials, 2019, 2, 4367-4376.	2.4	37
33	High-frequency electromagnetic properties of the manganese ferrite nanoparticles. Journal of Applied Physics, 2015, 117, .	1.1	34
34	Static and Dynamic Magnetization of Gradient FeNi Alloy Nanowire. Scientific Reports, 2016, 6, 20427.	1.6	28
35	Carbon black-supported FM–N–C (FM = Fe, Co, and Ni) single-atom catalysts synthesized by the self-catalysis of oxygen-coordinated ferrous metal atoms. Journal of Materials Chemistry A, 2020, 8, 13166-13172.	5.2	27
36	Templateâ€Free Formation of Uniform Fe <sub>3</sub> O <sub>4</sub> Hollow Nanoflowers Supported on Reduced Graphene Oxide and Their Excellent Microwave Absorption Performances. Physica Status Solidi (A) Applications and Materials Science, 2018, 215, 1701049.	0.8	26

#	Article	IF	CITATIONS
37	Chemical Synthesis of High-Stable Amorphous FeCo Nanoalloys with Good Magnetic Properties. Nanomaterials, 2018, 8, 154.	1.9	26
38	Doping and interface engineering in a sandwich Ti <sub>3</sub> C <sub>2</sub> T <sub><i>x</i></sub> /MoS <sub>2â^'<i>x</i></sub> P <sub><i>x</i></sub> heterostructure for efficient hydrogen evolution. Journal of Materials Chemistry C, 2022, 10, 4140-4147.	2.7	26
39	Facile synthesis of various Co3O4/bio-activated carbon electrodes for hybrid capacitor device application. Journal of Alloys and Compounds, 2022, 891, 161967.	2.8	22
40	Carbon Fibers Embedded with Aligned Magnetic Particles for Efficient Electromagnetic Energy Absorption and Conversion. ACS Applied Materials & amp; Interfaces, 2021, 13, 5266-5274.	4.0	21
41	Clarifying the preferential occupation of Ga <sup>3+</sup> ions in YAG:Ce,Ga nanocrystals with various Ga <sup>3+</sup> -doping concentrations by nuclear magnetic resonance spectroscopy. Journal of Materials Chemistry C, 2016, 4, 10691-10700.	2.7	20
42	Solvothermal synthesis and good microwave absorbing properties for magnetic porous-Fe3O4/graphene nanocomposites. AIP Advances, 2017, 7, .	0.6	19
43	Plasmon-Enhanced Oxygen Evolution Catalyzed by Fe <sub>2</sub> N-Embedded TiO <sub><i>x</i></sub> N <sub><i>y</i></sub> Nanoshells. ACS Applied Energy Materials, 2020, 3, 146-151.	2.5	18
44	Hydrogen Passivation of M–N–C (M <b>=</b> Fe, Co) Catalysts for Storage Stability and ORR Activity Improvements (Adv. Mater. 38/2021). Advanced Materials, 2021, 33, 2170300.	11.1	17
45	Multiple reflection and scattering effects of the lotus seedpod-based activated carbon decorated with Co3O4 microwave absorbent. Journal of Colloid and Interface Science, 2021, 602, 344-354.	5.0	16
46	Non-classical hydrogen storage mechanisms other than chemisorption and physisorption. Applied Physics Reviews, 2022, 9, .	5.5	16
47	Dielectric parameters of activated carbon derived from rosewood and corncob. Journal of Materials Science: Materials in Electronics, 2020, 31, 18077-18084.	1.1	14
48	Multiscale influence of trace Tb addition on the magnetostriction and ductility of <mml:math xmlns:mml="http://www.w3.org/1998/Math/MathML"&gt;<mml:mrow><mml:mo>â@©</mml:mo><mml:mn>100&lt; oriented directionally solidified Fe-Ga crystals. Physical Review Materials, 2019, 3, .</mml:mn></mml:mrow></mml:math 	/monostmn>	·≺not≄nl:mo>âC
49	3-D hierarchical urchin-like Fe3O4/CNTs architectures enable efficient electromagnetic microwave absorption. Materials Science and Engineering B: Solid-State Materials for Advanced Technology, 2022, 281, 115721.	1.7	14
50	Controlled Morphologies and Intrinsic Magnetic Properties of Chemically Synthesized Large-Grain FeCo Particles. Journal of Superconductivity and Novel Magnetism, 2015, 28, 1863-1869.	0.8	13
51	Synthesis and Physical Properties of Mn Doped ZnO Dilute Magnetic Semiconductor Nanostructures. Journal of Superconductivity and Novel Magnetism, 2011, 24, 699-704.	0.8	12
52	Spatial porosity design of Fe–N–C catalysts for high power density PEM fuel cells and detection of water saturation of the catalyst layer by a microwave method. Journal of Materials Chemistry A, 2022, 10, 7764-7772.	5.2	11
53	Roles of L1 ordering in controlling the magnetic anisotropy and coercivity of (111)-oriented CoPt ultrathin continuous layers in CoPt/AlN multilayer films. Journal of Applied Physics, 2011, 110, .	1.1	9
54	High-Frequency Absorption of the Hybrid Composites with Spindle-like Fe <sub>3</sub> O <sub>4</sub> Nanoparticles and Multiwalled Carbon Nanotubes. Nano, 2016, 11, 1650097.	0.5	8

#	Article	IF	CITATIONS
55	Effect of aspect ratio on microstructure and magnetic properties of spinel CoFe2O4 nanowire arrays. Applied Physics A: Materials Science and Processing, 2011, 105, 177-181.	1.1	7
56	Magnetic and Microwave Absorption Properties of Core/Shell FeCo-Based Nanocomposites Synthesized by a Simple Wet Chemical Method. IEEE Transactions on Magnetics, 2011, 47, 3456-3459.	1.2	6
57	Structural Formation and Improved Performances of Chemically Synthesized Composition-Controlled Micron-Sized Fe100â^'x Co x Particles. Journal of Superconductivity and Novel Magnetism, 2016, 29, 417-422.	0.8	5
58	Spin reorientation transition in (111) textured L10 CoPt layers. Applied Physics A: Materials Science and Processing, 2012, 109, 69-73.	1.1	4
59	Size Influence to the High-Frequency Properties of Granular Magnetite Nanoparticles. IEEE Transactions on Magnetics, 2014, 50, 1-4.	1.2	4
60	Facile Synthesis of Amorphous MoCo Lamellar Hydroxide for Alkaline Water Oxidation. ChemSusChem, 2022, 15, .	3.6	4
61	Curie temperatures of CoPt ultrathin continuous films. Applied Physics A: Materials Science and Processing, 2012, 107, 519-523.	1.1	3
62	Electromagnetic Properties of Co/Co <sub>3</sub> O <sub>4</sub> /Reduced Graphene Oxide Nanocomposite. IEEE Transactions on Magnetics, 2014, 50, 1-4.	1.2	2
63	Photocatalytic activity of Fe3O4/Bi2MoO6 composite in Rhodamine B decomposition. Journal of Applied Physics, 2015, 117, 17D709.	1.1	2
64	Photocatalytic Activity of Magnetically Retrievable Bi <sub>2</sub> WO <sub>6</sub> /ZnFe <sub>2</sub> O <sub>4</sub> Adsorbent for Rhodamine B. IEEE Transactions on Magnetics, 2014, 50, 1-4.	1.2	1
65	Temperature-Driven Spin Reorientation Transition in CoPt/AlN Multilayer Films. Journal of Nanomaterials, 2012, 2012, 1-7.	1.5	Ο
66	Magnetically induced abnormal grain growth in pure nickel. Materials Science and Technology, 2019, 35, 1533-1538.	0.8	0